Dynamic Performance Analysis of Solar Organic Rankine Cycle with Thermal Energy Storage

Shuai Li[a] , Hongjie Ma[b*] ,Weiyi Li[a]
[a] Key Laboratory of Efficient Utilization of Low and Medium Grade Energy, MOE, Tianjin University, Tianjin 300350, China
[b] Institute of Industrial Research, University of Portsmouth, Portsmouth, Hampshire PO1 2EG, United Kingdom

Highlights

A dynamic model of SORC was developed considering time-varying solar radiation.
The factor *FSR* was defined to reflect the effect of TES on dynamic impact.
Resonance occurs by the combined effect of TES capacity and solar disturbance.

Abstract

This paper discusses the dynamic performance in a small-scale solar organic Rankine cycle (SORC) with thermal energy storage (TES) considering solar disturbance. A dynamic model of SORC is developed. The factor *FSR* (Fluctuation Suppression Ratio) is defined to reflect the effect of TES on suppressing the dynamic impact. The dynamics of the SORC are found to contain resonance characteristics. With the interaction between solar disturbances and system thermal inertia (mainly determined by TES capacity), the energy superposition could cause dynamic resonance. In order to study the dynamic performance of the SORC, the influence factor including TES capacity, solar fluctuation (period, amplitude, average solar) and evaporation temperature were analysed, while FSR and the total system efficiency were the indicators which represent the system stability and performance respectively. The simulation result shows that within a certain solar period, there is a specific TES capacity range leading to resonance. The proper TES capacity should be selected according to local solar fluctuations to effectively suppress dynamic impact in the initial design phase.

Keywords:
ORC, Thermal Energy Storage, Dynamic performance, Disturbance, Solar energy

1 Introduction

Fossil fuel shortage and global warming are becoming severe. Moreover, with the increasing energy demand, electricity price has increased by about 12% in the past decade [1, 2]. Solar energy has great potential to produce electricity as a clean energy. A number of researchers have worked on improving solar thermodynamic cycles. The applications of ORC using renewable energy to the electricity generation have attracted much attention. ORC has been proposed because of its high efficiency in recovering the low-grade heat, such as geothermal energy, ocean thermal energy, waste heat, and solar energy [3][4]. ORC exhibits great flexibility, high safety, good reliability, and simplicity [5]. Solar organic Rankine cycle (SORC) has been proposed as an effective measure to use solar energy [6].

Most research about SORC is simulated to analyze performance using the steady-state model [7, 8]. The studies include the analysis about working fluid, solar collector[9], type of system structure, optimization of system parameters etc. Ksayer [10] investigated the influence

Corresponding author: Hongjie Ma. Tel: +44 7421307789
Email: hongjie.ma@port.ac.uk

of the evaporator temperature in SORC utilizing the hot water (393.15K) as heat source instead of real solar radiation . He et al. [11] developed the SORC by TRNSYS, and investigated the system efficiency and heat loss from the types of working fluid, flow rate, evaporation temperature, and TES capacity.

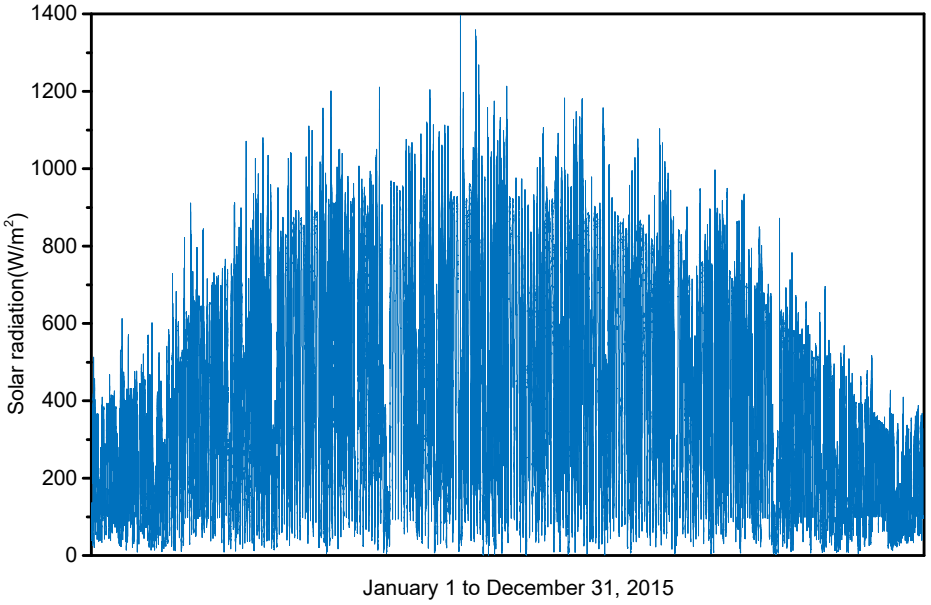

Fig. 1 Real-time solar radiation in 2015 at Fort Peck, in the United States

However, real solar radiation is unstable heat source that is easily affected by weather and season. The instability of solar energy is an important factor restricting the efficient utilization. As shown in Fig. 1, there is a huge fluctuation in the solar radiation in the year (up to 779.5 W/m^2 per minute), taking the Fort Peck region of the United States as an example[12]. Solar is fluctuated by seasonal alternation, day and night alternation, and the weather changes (dusky, sunny, and cloudy). The actual operation of the SORC is often under off-design conditions. Especially in some disturbances (such as cloud interference), the dynamic impact will greatly influence the system performance, and even cause damage [9] . Some studies have been focused on the dynamic model of the SORC. Hajabdollahi et al.[13] optimized the RSORC by hourly analysis considering evaporator pressure, condenser pressure, refrigerant mass flow rate, number of solar panel (solar collector), and storage capacity. Bamgbopa et al. [14] found that the evaporator and the condenser are critical components of the simplified transient modeling using R245fa.

However, there are few research on the dynamic performance of SORC under solar disturbance. Zhao et al. [15] investigated the dynamic performance of SORC without TES on the off-design condition caused by cloud disturbance. They found that the output power shows a high sensitivity to the variation of heat source. As TES is a critical component of SORC to reduce the dynamic impact, the dynamic performance of SORC with TES is studied in this paper.

In order to ensure the normal operation of SORC, TES is necessary in the system. TES was integrated into SORC to reduce the dynamic impact caused by time-varying solar radiation [16]. TES has two significant advantages. First, TES can achieve peak load shifting of the output power to meet the requirements. Solar energy could be stored during the day and release it to generate electricity at night [17]. Therefore, in the large-scale SORC, the thermal storage system usually has a complex design [18][19] and uses phase-change storage[20] materials to ensure high-density energy. Second, TES provides solar energy during periods of cloudy

weather to ensure the stable operation of the system [21]. The sudden change in input power negatively affects the expander and consequently the stability of the system [22].

In this paper, a dynamic model of a small-scale SORC system is developed. Dynamic performance of SORC is analyzed on the off-design condition caused by solar disturbances. The factor FSR(Fluctuation Suppression Ratio) is defined to reflect the effect of TES on suppressing dynamic impact. In order to study the dynamic performance of the SORC, the influence factor including TES capacity, solar fluctuation (period, amplitude, average solar) and evaporation temperature are analyzed, while FSR and the total system efficiency were the indicators which represent the system stability and performance respectively.

2 Performance simulation methods

The dynamic model of small-scale SORC system consists of two parts: solar collector system and basic ORC. The system includes solar collector, TES, pump, evaporator, expander, condenser, and pump. The evaporator is the thermal link between the two parts.

In the SORC (Fig. 2), water is the medium in the solar collector system, while R245fa (critical pressure: 3.651MPa, critical temperature: 427.16K, ODP: 0, GWP: 1030) is the working fluid in the basic ORC. Water absorbs heat from the solar collector and transfers heat to the organic working fluid through the evaporator. R245fa absorbs heat in the evaporator, and then goes into the expander to generate power. Then the low-pressure organic steam from the outlet of the expander goes into the condenser to release heat. Finally, the organic working fluid is pressed by the pump to the evaporator to absorb heat again to complete the cycle.

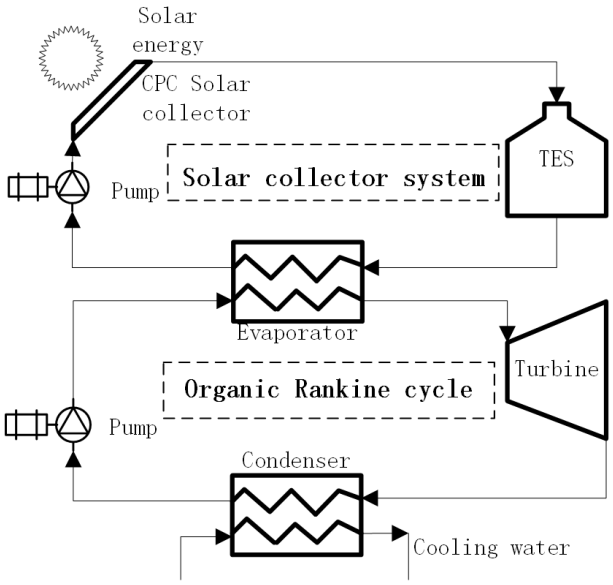

Fig. 2 Schematic diagram of the SORC power system

2.1 Component models

2.1.1 The model of solar collector

Solar energy, which is absorbed by solar collector, mainly includes the direct radiation and scattered radiation. The direct radiation is the solar radiation spread by straight line, which is mainly related to the solar altitude angle, altitude azimuth, and latitude in the place. The scattered radiation refers to the solar through the atmosphere, horizon, water vapor and so on. The radiation on the solar collector can be shown as the following formula [13]

$$\dot{I}_t = \left(\dot{I}_b + \dot{I}_d \frac{\dot{I}_b}{\dot{I}_h}\right) R_b + \dot{I}_d \left(1 - \frac{\dot{I}_b}{\dot{I}_h}\right) \left(\frac{1+\cos\beta}{2}\right) \left(1 + \sqrt{\dot{I}_b/\dot{I}_h} \sin^3\left(\frac{\beta}{2}\right)\right) + \dot{I}_h \rho_g \left(\frac{1-\cos\beta}{2}\right) \quad (1)$$

$\dot{I}_b$ means the direct radiation; $\dot{I}_d$ means the scattering radiation; $\dot{I}_h$ means the sum of direct radiation and the scattering radiation; R_b means the ratio of actual surface radiation and the horizontal radiation; β is the slant angle of collector; ρ_g means the environment reflection coefficient.

The heat absorption capacity of solar collector can be represented as the function of hot water mass flow rate ($\dot{m}_{htf}$) and collector heat transfer rate ($\dot{H}_{colletor}$) in heat collection cycle:

$$\dot{Q}_{colletor} = \dot{m}_{htf} \times \dot{H}_{colletor} \quad (2)$$

The heat transfer rate of solar collector ($\dot{H}_{colletor}$) can be calculated by the total solar radiation of inclined plane in unit area ($\dot{I}_t$), the effective heat exchange area ($A_{collector}$) and the collector efficiency ($\eta_{collector}$):

$$\dot{H}_{colletor} = \eta_{collector} \times \dot{I}_t \times A_{collector} \quad (3)$$

The collector efficiency is:

$$\eta_{collector} = a_0 - a_1 \times \frac{\Delta T}{\dot{I}_t} - a_2 \times \frac{\Delta T^2}{\dot{I}_t} \quad (4)$$

a_0, a_1 and a_2 is the constant of the equation of solar collector efficiency. a_0 means the maximum efficiency of the collector; a_1 and a_2 means the first and the second heat loss coefficient, respectively. ΔT means the temperature difference between the average temperature of working fluid and the environment temperature in the collector. The efficiency coefficient is shown in Table 1. The collector efficiency of the model is shown in Fig. 3. The horizontal axis formula is $x = T_{average} - T_{environment}/I_t$. Herein $T_{average}$ means the average temperature of the collector, $T_{environment}$ means the environment temperature, I_t is the solar radiation intensity. The design parameter of CPC collector is shown in Table 2.

Table 1 Efficiency coefficient

a_0	a_1（W/m^2 • K）	a_2（W/m^2 • K）
0.6831	0.2125	0.001672

Table 2 Design parameter of CPC collector

Area	Tilt angle	Azimuth angle
5.75 m^2	45°	0°

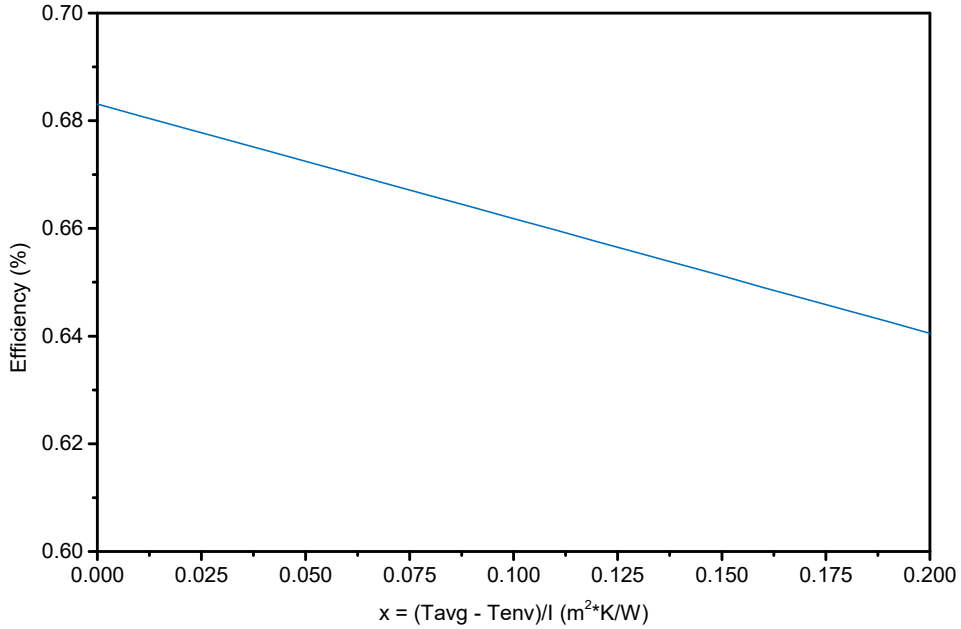

Fig. 3 Efficiency of CPC collector

2.1.2 Thermal energy storage model

The working fluid comes into the TES after absorbing the heat in the solar collector. According to the first law of thermodynamics, the temperature change of each step inside TES is shown as below:

$$T_{stor}(t+1) = T_{stor}(t) + (\sum \dot{H}_{in}(t) - \sum \dot{H}_{iout}(t) - \dot{H}_{los}(t)) \frac{3600\tau}{m_{stor}C_P} \quad (5)$$

τ means the time step; $m_{stor}C_P$ means the heat storage capacity of tank; $\dot{H}_{los}$ means the heat loss to the environment.

$$\dot{H}_{los} = (UA\Delta T)_{stor} \quad (6)$$

U means the overall coefficient of heat transfer, 1W/m^{2}K; A means the heat transfer surface area of TES; ΔT means the temperature difference between inner and outside of the TES. The heat transfer surface area calculation of TES is based on capacity and the height-diameter ratio r (the ratio of height and diameter), which is shown as follow:

$$A_{stor} = (\pi r)^{1/3}[4m_{stor}/\rho]^{2/3} \quad (7)$$

ρ is the medium density of TES; r is the height-diameter ratio of the heat reservoir and take as 2.5.

2.1.3 Heat exchangers

While large-scale ORC usually use two-phase zone exchangers, small-scaled ORC

preferably use single-phase heat exchange in the heat exchange model.

The heat exchanger is divided into (N-1) cells, N is 10. Heat transfer coefficient, fluid volume, and fluid mass are as follows:

$$A_i = \frac{A}{N-1};\ V_i = \frac{V}{N-1};\ M_i = \frac{M_W}{N-1} \tag{8}$$

The mass balance is calculated by:

$$\sum_1^{N-1} \frac{dM_i}{dt} = \dot{M}_1 - \dot{M}_{N-1} \tag{9}$$

M_i is the fluid mass, defined as:

$$M_i = \bar{\rho}_i \cdot V_i \tag{10}$$

$$\bar{\rho}_i = \frac{\rho_i + \rho_{i+1}}{2} \tag{11}$$

The energy conservation is given by:

$$A\rho \frac{dh}{dt} + \dot{M} \frac{dh}{dx} = A \frac{dp}{dt} + \frac{d\dot{Q}}{dx} \tag{12}$$

The heat balance over the wall is given by:

$$c_w \cdot M_W \cdot \frac{dT_{W,i}}{dt} = A \cdot (\dot{q}_{f,i} + \dot{q}_{hf,i}) \tag{13}$$

$\dot{q}_{f,i}$ is the heat fluxes of working fluid, $\dot{q}_{hf,i}$ is the heat fluxes of hot fluid, defined as respectively:

$$\dot{q}_{f,i} = U_{f,i} \cdot (T_{f,i} - T_{W,i}) \tag{14}$$

$$\dot{q}_{hf,i} = U_{hf,i} \cdot (T_{hf,i} - T_{W,i}) \tag{15}$$

Table 3 Design parameter of heat exchanger

Parameter	Value	Parameter	Value (W/m^{2}K)
M_{hw}	1kg/s	$U_{f,l}$	260
$T_{condenser}$	298.15K	$U_{f,tp}$	900
U_{hf}	1000	$U_{f,v}$	360

2.1.4 Pump model

The model is only suitable for the incompressible fluid. According to the first law of thermodynamics, the pump model is calculated by:

$$\dot{m}\left(h_{in} + \frac{1}{2}v_{in}^2\right) = \dot{m}\left(h_{out} + \frac{1}{2}v_{out}^2\right) + W \tag{16}$$

which can be simplified as:

$$\dot{m}(h_{out} - h_{in}) = (p_{out} - p_{in})/\rho \tag{17}$$

h_{out} and h_{in} mean the inlet enthalpy and outlet enthalpy of the pump, respectively. p_{out} and p_{in} mean the outlet and the inlet pressure of the pump, respectively. The work consumption for pump is shown as follow:

$$\frac{\dot{W}_{pump}}{\dot{m}} = \frac{h_{out} - h_{in}}{\eta} = \frac{p_{out} - p_{in}}{\eta\rho} \tag{18}$$

$$\dot{W}_{pump} = \frac{\dot{m} \cdot \Delta p}{\rho\eta} \tag{19}$$

η means the pump efficiency, ρ means the working fluid density.

The outlet enthalpy in the pump is shown as follow:

$$\dot{H}_{out} = \dot{H}_{in} + \dot{W}_{pump} \tag{20}$$

The characteristic time is used to delay the pump outlet flow rate. The first order transfer function and time constant are used to represent the transfer function in the model. The formula is:

$$\frac{y_{(s)}}{u_{(s)}} = \frac{1}{\tau s+1} \tag{21}$$

In the model, the actual flow value of the pump equals to the product of the given maximum flow value and the given controlling value.

2.1.5 Expander model

In expander module, the pressure drop of fluid is mainly regulated by adjusting the mass flow of the working fluid. The output power can be represented as:

$$\dot{W}_t = \dot{m}_{wf}(h_3 - h_4)\eta_{turbine} \tag{22}$$

$\eta_{turbine}$ means the expender efficiency, which is 65%; h_4 mean the outlet enthalpy of the expander, h_3 means the inlet enthalpy of the expender.

2.1.6 Control strategy

The PI controller is used to ensure the stable operation of the system. The control strategy in this paper is to define the evaporation temperature and superheat as constant. Evaporation temperature as a critical condition affected the efficiency and normal operation. In order to cooperate with the solar condition, the pump speed is adjusted, to control the working fluid flow, and then ensure the constant of superheat.

The control signal is expressed as the equation:

$$m(t) = e(t) + \frac{k}{T_i}\int_0^t e(t)\,dt \tag{23}$$

Where, k is the proportional gain, $e(t)$ is the error between the actual value and the set point, T_i is the integral time constant.

In the PI controller, according to the control deviation between the actual input signal and the set value, adjustable ratio P and integral I and output signal is linear. k and T_i can be adjusted to optimize. The two parameters affected the stable time and vibration amplitude when the solar changed.

2.2 System thermal model

Thermal efficiency η_{th} is as follow:

$$\eta_{th} = \frac{W}{Q_{eva}} = \frac{m\times(h_{turbine,in}-h_{turbine,out})\times\eta_{turbine}}{m\times(h_{eva,out}-h_{eva,in})} \tag{24}$$

W is the output power; Q_{eva} is the absorption heat in evaporator; m is the mass flow rate; $\eta_{turbine}$ is the expander efficiency, 65%.

The total system efficiency η_{sys} is as follow:

$$\eta_{sys} = \eta_{collector} \times \eta_{th} \tag{25}$$

$\eta_{collector}$ is the solar collector efficiency, which is calculated by formula (4).

2.3 System simulation and data generation

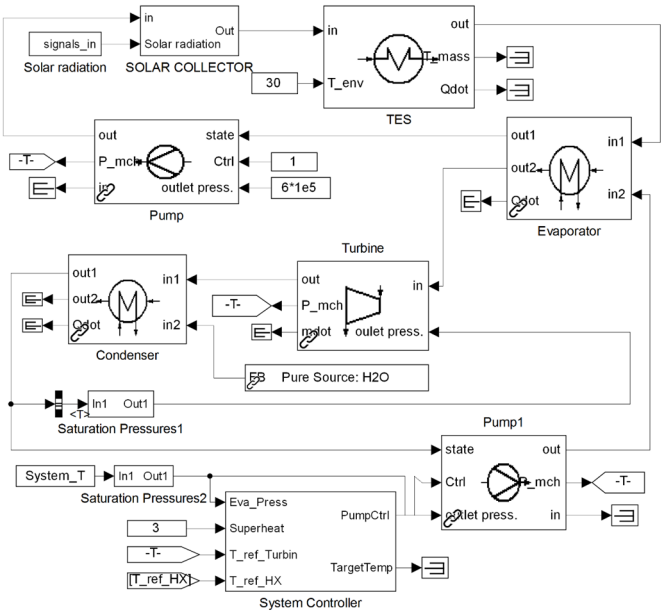

Fig. 4 Dynamic simulation model of SORC

The dynamic model of SORC is built in Matlab/Simulink (shown as Fig. 4). In the running process, the data of working fluid can be observed through the display module. In the setting interface, the information including temperature, flow rate, entropy, and enthalpy can be displayed in real time. The specific state and continuous state of a certain point can be monitored in real time. Finally, physical and thermodynamic parameters of all state points can be obtained after the simulation, and recorded in the corresponding file.

3 Results and discussion

3.1 Dynamic resonance in the disturbed condition

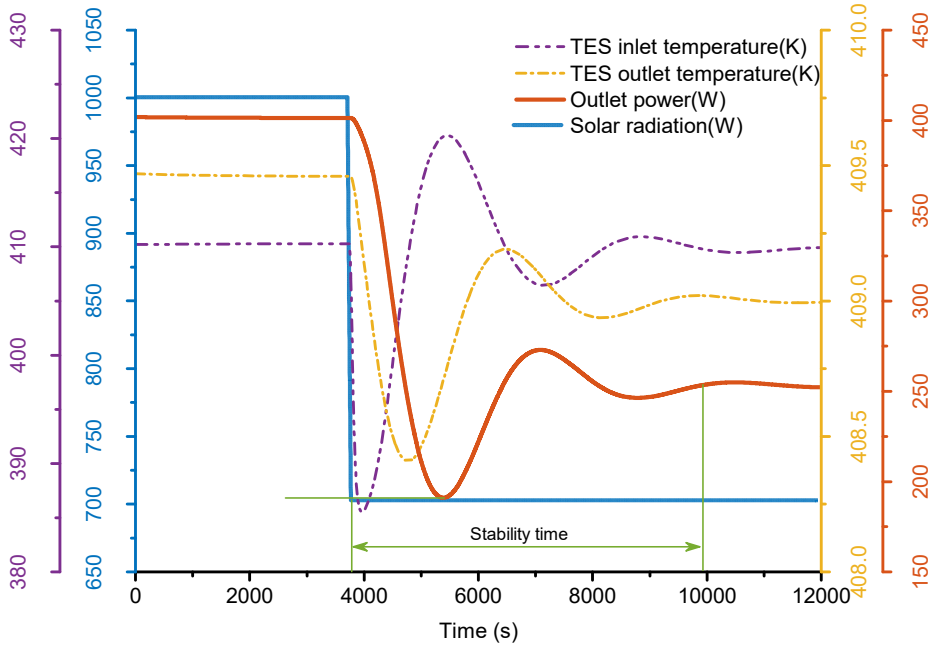

Fig. 5 Dynamic responses of SORC under disturbance condition

When the solar radiation decreases from 1000W/m^2 to 700W/m^2 in 3740s, PI controller reduces the flow rate of working fluid to reach the new set point (shown in Fig. 5). During the stability time, the output power and temperature of TES fluctuate due to flow regulation, and eventually reach equilibrium.

The residence time is defined to the phase delay between it and solar disturbance. It is caused by the system thermal inertia. The stability time is defined as the time when the system is adjusted to stabilize after disturbance occurs. When the system is running, the control parameters in the actual system operation are usually kept constant. Therefore, the stability time is determined by solar disturbances and system thermal inertia.

So, the fluctuation of output power during the stability time is directly impacted by solar disturbance and system thermal inertia. As largest heat capacity of the component, the system thermal inertia is mainly determined by the TES capacity. Therefore, with the combined effect of solar continuous disturbances and TES capacity, the fluctuation of output power will be superimposed, which may lead to dynamic resonance on a specific condition (shown as Fig.6 and Fig.7).

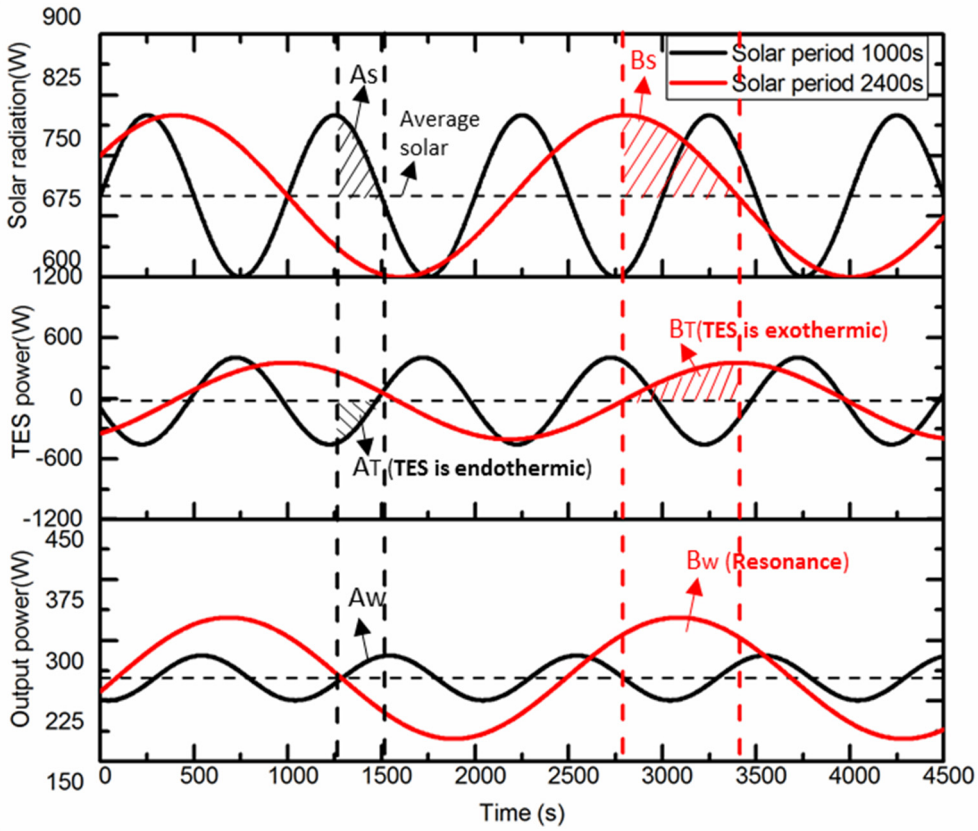

Fig. 6 Dynamic process of system when the period of solar disturbance changed. (TES power=$Q_{outlet} - Q_{inlet}$. TES power<0, TES is endothermic; TES power>0, TES is exothermic.)

Solar continuous disturbances can be abstracted as a sine wave, shown as Fig.6. When the period of solar fluctuation changes, the fluctuation of TES storage power and output power also changes significantly. In Fig.6, when the instantaneous solar radiation is higher than the average solar (such as A_S), TES is endothermic (A_T<0), absorbing the excess heat. This fact cushions the dynamic impact of the system. However, it is worth noting that the amplitude of output power increases significantly when the solar period is 2400 s. At this time, while the instantaneous solar radiation (B_S) is higher than the average, TES is exothermic (B_T>0), increasing the amplitude of output power. This fact causes the enhancement of the system dynamic impact. Therefore, with the interaction between a specific solar continuous disturbances and TES, the energy superposition could cause dynamic resonance.

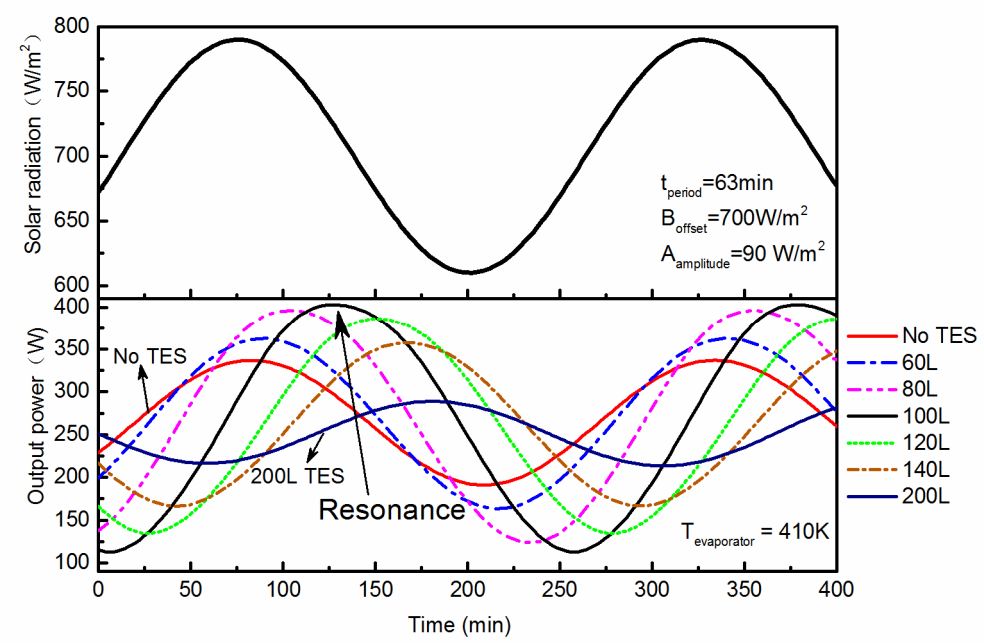

Fig. 7 Effect of TES capacity on dynamic resonance

From the above analysis, the dynamic resonance of the output power is mainly determined by solar disturbance and the system thermal inertia. The thermal inertia is mainly affected by the TES capacity. It means that resonance occurs on the collective effect of a certain solar constantly changing and a specific TES capacity. Fig. 7 shows that resonance occurs when TES capacity is 100L.When leaving the resonant region, TES has the great impact on suppressing the fluctuation of output power.

3.2 Definition of fluctuation suppression ratio

For analyzing the resonance phenomenon which is found in the above section, Fluctuation Suppression Ratio (FSR) is defined to reflect the suppression effect of TES to the system. FSR= A_L/A_S, where A_L stand for amplitude with a certain TES, where A_S stands for amplitude without TES. Fig. 8 shows the definition of FSR. The waves of SORC with 300L TES are significantly less than the system without TES. The smaller value of FSR represents the better effect of TES on the fluctuation suppression. FSR<1 indicates that TES has positive effect on suppressing fluctuations, while FSR>1 indicates that TES exacerbates the system instability. FSR should be one of the system dynamic indexes.

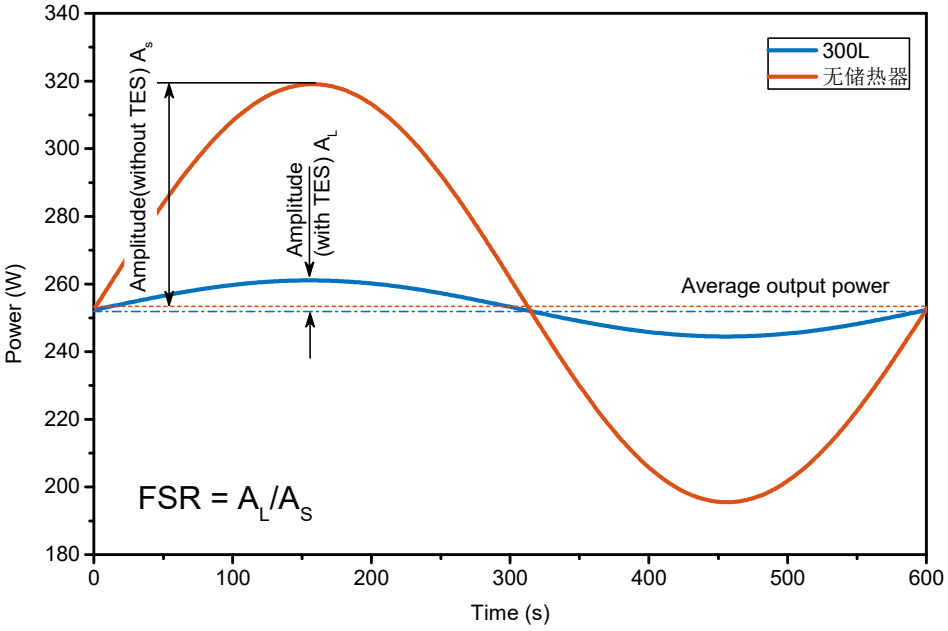

Fig. 8 Definition of Fluctuation Suppression Ratio

3.3 Effects of TES on dynamic resonance

In this paper, the influence factor of dynamic resonance is analyzed. TES which lead to large thermal inertia, has great influence on the dynamic performance. Meanwhile, solar disturbances are the main external factors that affect the dynamic performance of the system, while evaporation temperature is the main internal factor affecting the performance of the system. Therefore, the effect of TES on system dynamic performance under different solar fluctuations (including period, amplitude, and average soar radiation) and evaporation temperature were analyzed. In addition, FSR and the total system efficiency, which represent the system stability and performance respectively, are selected to the indicators of dynamic performance in SORC.

3.3.1 Influence of different solar disturbance

The real solar radiation is constantly fluctuating (as Fig. 9), which is affected by clouds, weather and so on. Numerous different waves compose the real solar. All of these waves can be decomposed into the superposition of sine wave with different amplitudes, periods and phases by Fourier transform. Therefore, the solar fluctuation is abstracted into a group of sine waves to study its impact on SORC.

As the solar fluctuations is abstracted into sine wave, the characters of solar are described to the following parameters: solar period (t_{period}), amplitude ($A_{amplitude}$) and average solar radiation (B_{offset}). The effect of these characters of solar and TES capacity on dynamic performance are analyzed in the following section.

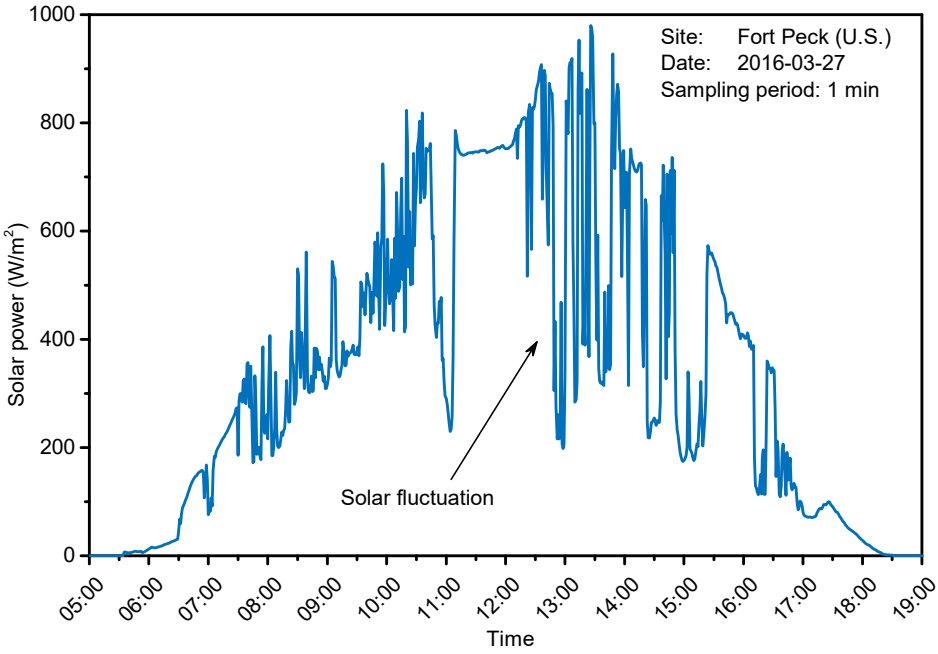

Fig. 9 Daily solar radiation in cloudy weather

3.3.1.1 Influence of different solar period in fluctuations

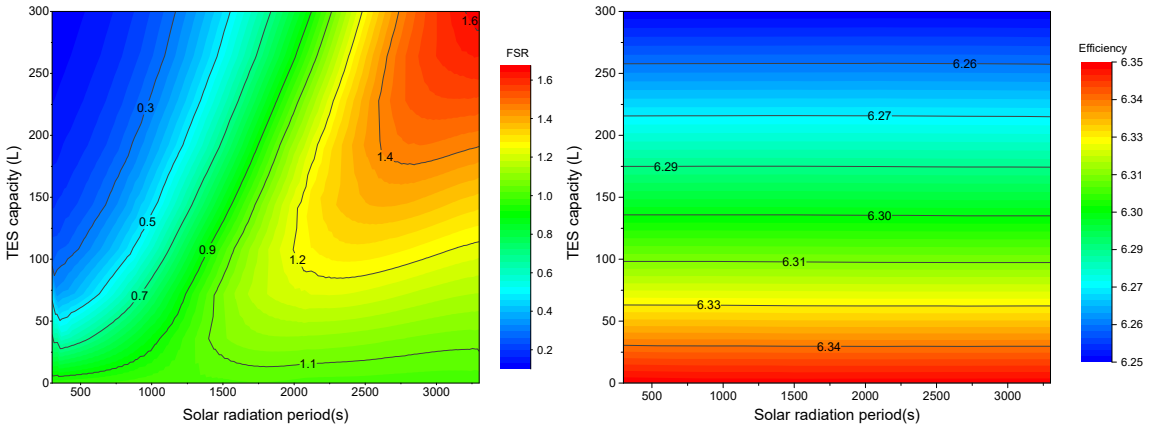

(a) (b)

Fig. 10 Effect of the solar radiation period on (a) FSR, (b) Total system efficiency ($A_{amplitude}$=100W/m^2, B_{offset}=700W/m^2, $T_{evaporator}$=406K)

FSR<1 indicates that TES has a positive effect on suppressing fluctuations of output power, while FSR>1 indicates that TES exacerbated fluctuations of output power. The region of FSR>1 is defined as the resonance region. Effect of the different solar period and TES capacity on FSR can be obtained from Fig. 10(a): 1) There are a resonance region of TES capacity, which is related to a certain solar period. For example, when the solar period is 1500s, the TES capacity belonging to the resonance region is 25L~100L, which aggravates the dynamic impact of the system. 2) When the solar period is longer, the TES capacity which is related to resonance is bigger and its range becomes wider. For example, when the solar period increases from 1500s to 2100s, the TES capacity about resonance region also increased from 25L~100L to 0~250L. 3) When out of the resonance region, the FSR significantly decreases with the increase of TES capacity, indicating more system stability with bigger TES. For example, when the TES capacity increases from 150L to 300L (solar period is 1500s, out of resonance region), FSR reduces from 0.85 to 0.46, which decreases by 45.88%. So, the resonance region should be avoided in design optimization.

Fig. 10(b) shows that the total system efficiency is not affected by the solar period. However, the larger TES capacity is, the lower total system efficiency is. This is because that the mixing of fluids at different temperatures in the TES increases the irreversible loss. In addition, the equal efficiency line is equidistant, indicating that there is linear relationship between TES capacity and total system efficiency.

3.3.1.2 Influence of the average solar radiation and amplitude in solar fluctuations

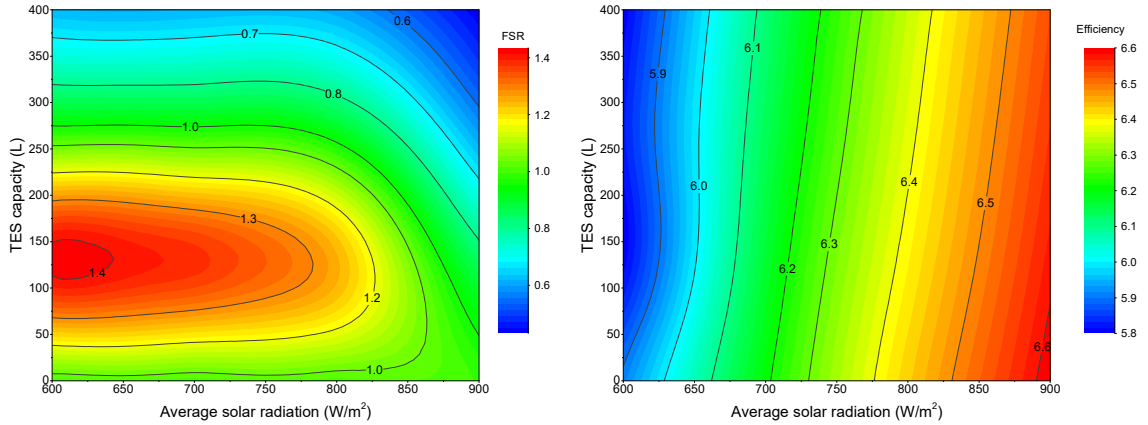

(a) (b)

Fig. 11 Effect of the different average solar radiation on (a) FSR, (b) Total system efficiency ($A_{amplitude}$=100W/m^2, t_{period}=1800s, $T_{evaporator}$=406K)

When the average solar radiation is increased, the heat absorbed in the system is increasing. In order to keep the system balance, the flow rate of working fluid is increased too. This fact results in an increase in the thermal inertia of the entire system. The increase of system thermal inertia causes FSR to decrease. Therefore, shown as Fig. 11(a), when the average solar is increased in the resonance region (FSR>1), FSR is decreased and the dynamic resonance is weakened on the system. Also, as shown in Fig. 11(b), with the increasing of the average solar radiation, the flow rate of working fluid increases, resulting to the increase of the total system efficiency.

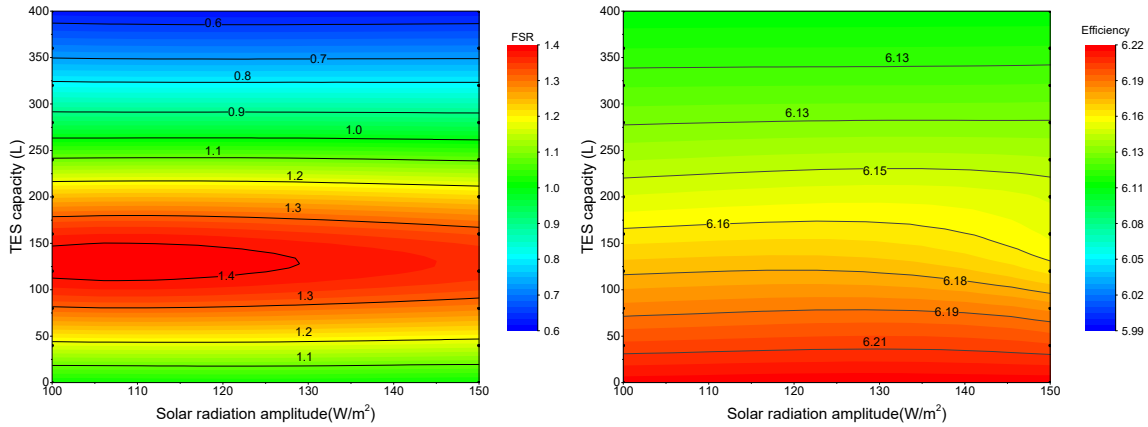

(a) (b)

Fig. 12 Effect of the solar amplitude on (a) FSR, (b) Total system efficiency (B_{offset}=700W/m^2, t_{period}=1800s, $T_{evaporator}$=406K)

In the resonance region (FSR>1), the solar amplitude has little impact on FSR. As shown in Fig.12 (a), when the solar amplitude is 100W/m^2~150W/m^2, the range of resonant volume of TES is same (0-250L). Similar to FSR, the amplitude of solar fluctuation also has little impact on the total system efficiency (as shown in Fig.12 (b)).

3.3.2 Influence of different evaporation temperatures

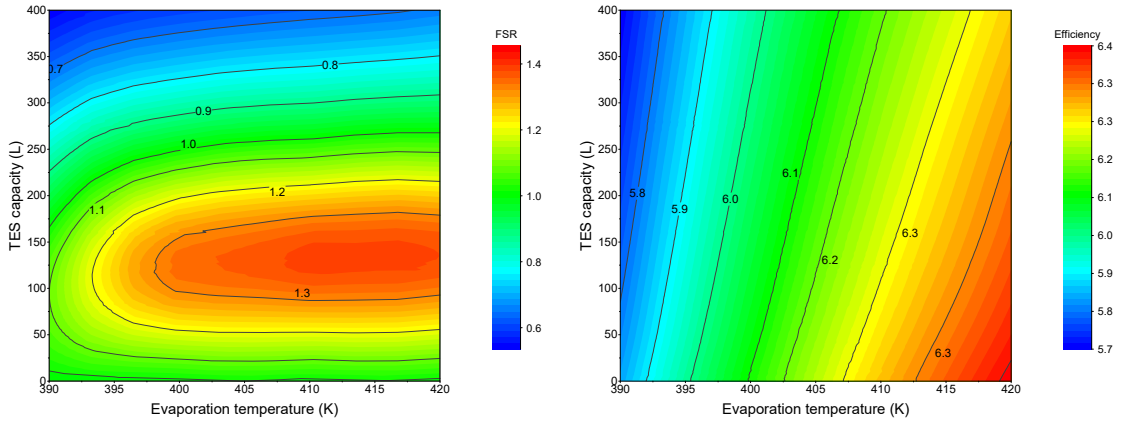

(a) (b)

Fig. 13 Effect of the different evaporation temperature on (a) FSR (b) Total system efficiency ($A_{amplitude}$=100W/m^2, t_{period}=1800s, B_{offset}=700W/m^2)

While the evaporation temperature is increased, the heat absorbed in the system is decreasing. In order to keep the system balance, the flow rate of working fluid is decreased. This fact results in a decrease in the thermal inertia of the entire system. Reduced thermal inertia of the system can cause FSR to increase. So, shown as Fig. 13(a), with the increasing of the evaporation temperature in the resonance region (FSR>1), FSR is increased and the dynamic resonance is strengthened on the system.

The influence of evaporation temperature on the total system efficiency is shown in Fig. 13(b). The results are as follows: 1) With the increasing of evaporation temperature, the total system efficiency increases. This is mainly because the improvement of the thermal efficiency in the ORC. 2) With the increasing of evaporation temperature, the increasing degree of the total system efficiency is decreased. It is because that the collector efficiency decreases with the increasing of evaporation temperature (shown in section 2.1.1), while the basic-ORC efficiency increases. Due to the interacting of the collector efficiency and basic-ORC efficiency, the increasing degree of the total system efficiency becomes smaller.

3.4 Discussion

The indicators that measure the output quality of the SORC system are made up of efficiency and fluctuation. According to the previous analysis, it can be seen that the evaporation temperature and TES capacity are important factors affecting the efficiency, and the solar radiation period and the TES capacity are important factors influencing the fluctuation. This means that the TES capacity has an impact on the both quality indicators of the SORC system output. So, the selection of TES capacity is important for the design of the SORC system. The effect of TES capacity on FSR and efficiency is given in Fig. 14 for a given solar radiation and evaporation temperature.

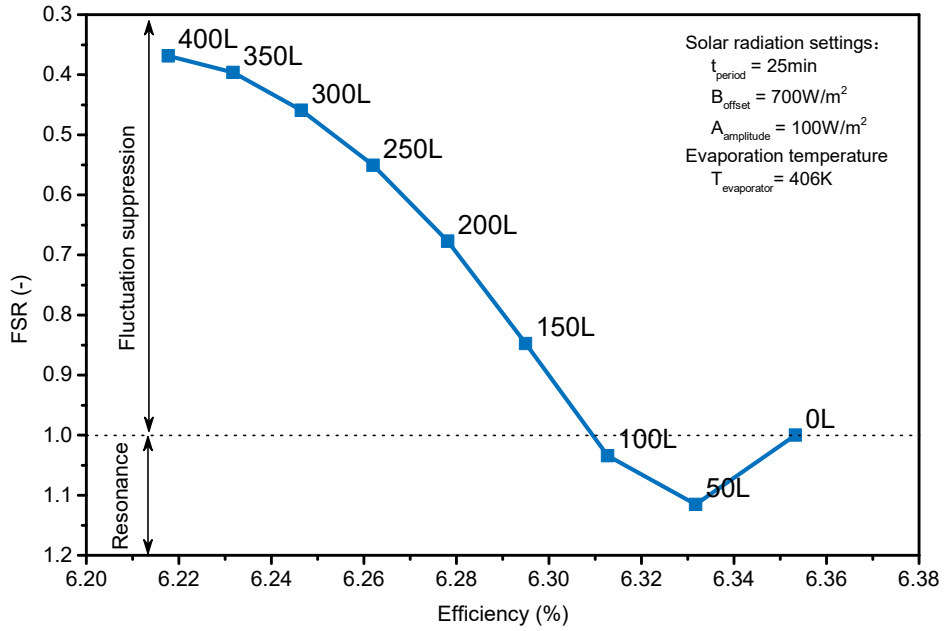

Fig. 14 Effect of the TES capacity on FSR and efficiency for a given solar radiation and evaporation temperature

As can be seen from the figure, the lower part of the figure is the resonance area(FSR>1). In this region, TES has a negative impact on both fluctuation and efficiency of the SORC system output. The reason for this phenomenon is described in the analysis of Fig. 5 and 6, with the combined effect of solar continuous disturbances and response delay of SORC system, the fluctuations of solar radiation power and TES power will be superimposed. This leads to the situation that the TES increases the output fluctuation of the system. At the same time, the absorption and desorption process in TES increase the irreversible loss of the system, which leads to the decrease of the system efficiency. So, this region needs to be avoided in the design.

For the fluctuating suppression region(FSR<1), the fluctuations of solar radiation power and TES power will offset each other. In this case, the suppression degree of the system output fluctuation depends on the capacity of the TES. As the example shown in Fig. 14, the FSR is improved by 50% and the efficiency is reduced by only 1% when the TES capacity increases from 100L to 300L. This means that increasing the capacity of the TES in this capacity range can significantly improve the output stability of the SORC system and have less impact on the system efficiency. However, with the further increase of TES capacity to 400L, the effect of TES on efficiency is basically the same but the effect on FSR is weakened. From this point of view, there is a cost-effective point for TES capacity selection.

4 Conclusions

A dynamic model of small-scaled SORC is developed. Different solar disturbances and system thermal inertia (mainly determined by TES capacity) can cause different amplitude and delay time in fluctuations of output power. With the interaction between a specific solar continuous disturbances and TES, the energy superposition could cause dynamic resonance. Dynamic resonance will enhance the system oscillation.

It is found that within a certain solar period, there is a specific TES capacity range leading to resonance. Besides, when the average solar radiation increases, dynamic resonance weakens on the system. However, in the resonance region, the solar amplitude has little impact on

dynamic resonance. In addition, when the evaporation temperature increases, dynamic resonance enhances on the system.

When the TES capacity increases, the total system efficiency will be slightly decreased. However, the total system efficiency increases with the increase of average solar radiation and evaporation temperature, while the period and amplitude of the solar fluctuation have little effect on the efficiency.

Therefore, the proper TES capacity should be selected according to local solar fluctuation to improve system stability. The control strategy is also one of the factors that affect the dynamic resonance, which will be studied in the future.

References

[1] Eurostat. Electricity prices for household consumers., 2013.

[2] Administration USEI. Average retail price of electricity to ultimate customers.

[3] Tchanche BF, Lambrinos G, Frangoudakis A, Papadakis G. Low-grade heat conversion into power using organic Rankine cycles--A review of various applications. Renewable and Sustainable Energy Reviews 2011;15(8):3963-79.

[4] Vetter C, Wiemer H, Kuhn D. Comparison of sub- and supercritical Organic Rankine Cycles for power generation from low-temperature/low-enthalpy geothermal wells, considering specific net power output and efficiency. APPL THERM ENG 2013;51(1–2):871-9.

[5] Nafey AS, Sharaf MA. Combined solar organic Rankine cycle with reverse osmosis desalination process: Energy, exergy, and cost evaluations. RENEW ENERG 2010;35(11):2571-80.

[6] Pei G, Li J, Ji J. Analysis of low temperature solar thermal electric generation using regenerative Organic Rankine Cycle. APPL THERM ENG 2010;30(8-9):998-1004.

[7] Lecompte S, Ameel B, Ziviani D, van den Broek M, De Paepe M. Exergy analysis of zeotropic mixtures as working fluids in Organic Rankine Cycles. ENERG CONVERS MANAGE 2014 2014-09-01;85:727-39.

[8] Feng Y, Hung T, Greg K, Zhang Y, Li B, Yang J. Thermoeconomic comparison between pure and mixture working fluids of organic Rankine cycles (ORCs) for low temperature waste heat recovery. ENERG CONVERS MANAGE 2015;106:859-72.

[9] Kim KH, Han CH. A Review on Solar Collector and Solar Organic Rankine Cycle (ORC) Systems. Journal of Automation and Control Engineering 2015:66-73.

[10] Ksayer EBL. Design of an ORC system operating with solar heat and producing sanitary hot water. Energy Procedia 2011;6:389-95.

[11] He Y, Mei D, Tao W, Yang W, Liu H. Simulation of the parabolic trough solar energy generation system with Organic Rankine Cycle. APPL ENERG 2012 2012-09-01;97:630-41.

[12] Augustine JA, DeLuisi JJ, Long CN. SURFRAD—A national surface radiation budget network for atmospheric research. B AM METEOROL SOC 2000;81(10):2341-57.

[13] Hajabdollahi H, Ganjehkaviri A, Mohd Jaafar MN. Thermo-economic optimization of RSORC (regenerative solar organic Rankine cycle) considering hourly analysis. ENERGY 2015;87:369-80.

[14] Bamgbopa MO, Uzgoren E. Quasi-dynamic model for an organic Rankine cycle. ENERG CONVERS MANAGE 2013 2013-08-01;72:117-24.

[15] Li Z, Zhao W, Shuai. D. Dynamic Performance of Solar Driven Organic Rankine Cycle Power System Under Cloud Disturbance. Journal of Tianjin University (Science and Technology) 2016;49(1):21-7.

[16] Baral S, Kim D, Yun E, Kim K. Experimental and Thermoeconomic Analysis of Small-Scale Solar Organic Rankine Cycle (SORC) System. ENTROPY-SWITZ 2015 2015-04-07;17(4):2039-61.

[17] Mu Z, Ding Y. Comparison and Performance Analysis of Heat Storage Equipment in Solar Heating System. Journal of Donghua University(English Edition) 2013 2013-06-30(03):197-201.

[18] Kuravi S, Trahan J, Goswami DY, Rahman MM, Stefanakos EK. Thermal energy storage technologies and systems for concentrating solar power plants. PROG ENERG COMBUST 2013;39(4):285-319.

[19] Casati E, Galli A, Colonna P. Thermal energy storage for solar-powered organic Rankine cycle engines. SOL ENERGY 2013;96:205-19.

[20] Chan CW, Ling-Chin J, Roskilly AP. Reprint of "A review of chemical heat pumps, thermodynamic cycles

and thermal energy storage technologies for low grade heat utilisation”. APPL THERM ENG 2013;53(2):160-76.
[21] Higgo AR, Zhang TJ. Characterization of a Compact Organic Rankine Cycle Prototype for Low-grade Transient Solar Energy Conversion. Energy Procedia 2015;69:1113-22.
[22] Fricker HW. Regenerative thermal storage in atmospheric air system solar power plants. ENERGY 2004;29(5-6):871-81.

Attached figures:

Attached tables: